

# Neural Window Decoder for SC-LDPC Codes

Dae-Young Yun, Hee-Youl Kwak, *Member, IEEE* Yongjune Kim, *Member, IEEE*, Sang-Hyo Kim, *Member, IEEE*, and Jong-Seon No, *Fellow, IEEE*

**Abstract**—In this paper, we propose a neural window decoder (NWD) for spatially coupled low-density parity-check (SC-LDPC) codes. The proposed NWD retains the conventional window decoder (WD) process but incorporates trainable neural weights. To train the weights of the NWD, we introduce two novel training strategies. First, we limit the loss function to target variable nodes (VNs) of the window, which prunes the neural network and accordingly enhances training efficiency. Second, we employ the active learning technique with a normalized loss term to prevent the training process from biasing toward specific training regions. Moreover, we develop a systematic method to derive non-uniform schedules from the training results by introducing trainable damping factors that reflect the relative importance of check node (CN) updates. By skipping updates with less importance, we can omit 41% of updates without performance degradation compared to the conventional WD. Lastly, we address the error propagation problem inherent in SC-LDPC codes by deploying a complementary weight set, which activates when an error is detected in the previous window. This adaptive decoding strategy effectively mitigates error propagation without requiring modifications to the code or decoder structure.

**Index Terms**—Low-density parity-check (LDPC) code, spatially coupled LDPC (SC-LDPC) code, window decoding, deep learning, neural decoder, decoding schedules, error propagation

## I. INTRODUCTION

THE advent of machine learning technologies has significantly impacted a broad area of technological fields. This impact is also prominent in the field of communications, spanning topics such as channel estimation [1], end-to-end communication [2], [3], and channel coding [4]–[7]. Particularly, the application of deep learning techniques to the channel coding problem has marked a significant milestone [7]. This pioneering work has introduced *neural decoders* that integrate the iterative decoding algorithms, such as belief propagation (BP) and min-sum (MS) algorithms, with deep neural networks. These neural decoders possess weights that are trained to attenuate decoding messages to mitigate the detrimental effect of short cycles.

In an effort to enhance the performance of neural decoders, a variety of machine learning techniques have been leveraged. Hyper-graph networks is incorporated into the neural network architecture to expand the model capacity [14]. Additionally,

the active learning technique [15], which involves the careful selection of effective training samples, and the pruning method [16] are utilized to improve the performance. Recently, the boosting learning technique is applied to address the error-floor issue of low-density parity-check (LDPC) codes [17]. Another distinctive approach to enhance the performance is simplifying the optimization problem. For instance, the concept of recurrent neural networks is employed in neural decoders [8], resulting in a reduction of the number of training parameters. Similarly, various weight sharing techniques such as spatial [10], protograph [11], and degree-based sharing [12] have been proposed. These techniques not only reduce training complexity and memory requirements but also improve decoding performance by reducing the optimization space of the neural network.

With these efforts, neural decoders have gained recognition for their practicality and have been applied to various code classes, including algebraic [13], [14], LDPC [10], [17], [18], generalized LDPC [19], and polar codes [20]. However, neural decoders have not yet been applied to one of the key counterpart of LDPC codes, the spatially-coupled LDPC (SC-LDPC) codes.

SC-LDPC codes, first introduced in [21], have attracted attention due to their threshold saturation effect, where their BP thresholds approach the optimal maximum a posteriori (MAP) thresholds of uncoupled block LDPC codes [22]. SC-LDPC codes are constructed by coupling  $L$  disjoint LDPC blocks in a repetitive structure. This recurrent form enables a unique decoding method known as window decoding [23]. The window decoder (WD) operates on a subgraph, referred to as a window, aiming to decode target variable nodes (VNs) in the first block. After decoding within the first window is complete, the process advances to the subsequent window and continues across all  $L$  blocks. Compared to the frame-wise decoding, which target all VNs, the WD offers advantages in terms of decoding latency, complexity, and memory requirements.

There are two important directions in the research of the WD. First, non-uniform scheduling is proposed to reduce decoding complexity [29]. Due to the unique structure of SC-LDPC codes, each CN update impacts the decoding process differently. The method in [29] measures the soft bit error rate (BER) estimation during the decoding process and omits CN updates that are expected to have a lesser impact on decoding. However, this method has a drawback in that it requires the computation of soft BERs during decoding, which introduces additional overhead. Second, an adaptive decoding strategy [30] and the doping method [31] are proposed to prevent error propagation (EP). The WD is particularly vulnerable to EP because decoding failures in preceding windows can negatively affect subsequent decoding, potentially leading to a

D.-Y. Yun and J.-S. No are with the Department of Electrical and Computer Engineering, INMC, Seoul National University, Seoul 08826, Korea (e-mail: dyyun@ccl.snu.ac.kr; jsno@snu.ac.kr).

Hee-Youl Kwak is with the Department of Electrical, Electronic and Computer Engineering, University of Ulsan, Ulsan 44610, South Korea. (e-mail: ghy1228@gmail.com).

Y. Kim is with the Department of Electrical Engineering at Pohang University of Science and Technology (POSTECH), Pohang, Gyeongbuk 37673, South Korea (e-mail: yongjune@postech.ac.kr).

S.-H. Kim is with the Department of Electrical and Computer Engineering, Sungkyunkwan University, Suwon 16419, South Korea (e-mail: iamshkim@skku.edu).

long chain of errors [24], [25]. The adaptive decoding strategy [30] varies iteration numbers, and the doping method [31] alters the decoding or encoding processes. Consequently, both approaches have drawbacks of modifying the existing code or decoding system.

### A. Main Contributions of This Paper

To improve key aspects of the WD such as performance, complexity, and robustness to EP, we propose a *neural window decoder* (NWD) for SC-LDPC codes. The NWD operates in the same manner as the conventional WD but incorporates trainable weights similar to neural decoders. To the best of our knowledge, this is the first neural decoder specifically designed for SC-LDPC codes. The novel features of the NWD include the following:

- 1) *Target-specific training*: We train the NWD using target-specific training, wherein the loss function only includes target VNs in the window. This approach aligns naturally with the operation of the WD and offers advantages in terms of neural network efficiency compared to conventional all-inclusive training that targets all VNs. By restricting the output nodes of the network to a subset of VNs, the network is pruned and simplified. This simplification facilitates more efficient training and results in enhanced decoding performance
- 2) *Bias prevention in training*: We introduce a new training method designed to prevent biases in training at low signal-to-noise ratio (SNR) points. Conventional neural decoders collect training samples across multiple SNR points, ranging from low to high, to cover the operational range. However, the loss term from high SNR regions is typically lower than that from low SNR regions, resulting in the training being biased on low SNR regions. To address this issue, we introduce a normalized loss term and the active learning technique that selectively collects training samples, thereby equalizing the importance of each SNR point.
- 3) *Neural non-uniform scheduling*: We introduce the neural non-uniform scheduling for the NWD. Specifically, we train an NWD with trainable damping factors, which determine the proportions between the current and previous updates in the CN outputs. A large damping factor indicates that the corresponding CN update is less significant. Based on this metric, we can achieve 59% reduction in CN updates without performance degradation compared to the conventional WD. Our scheduling method is pre-determined and does not require additional computation during decoding, offering an advantage over the conventional scheduling method [29].
- 4) *Adaptive NWD to mitigate EP*: We propose an adaptive NWD scheme to mitigate EP. We collect training samples that induce EP and use these to train so called breakwater weight set for scenarios where EP occurs. When a decoding failure in the previous window is declared, the adaptive NWD scheme employs the breakwater weight set, otherwise, it employs the plain weight set. The proposed adaptive scheme successfully decreases the probability of

---

### Algorithm 1 Proposed Neural Window Decoder (NWD)

---

**Input:** Window size  $\bar{W}$ , target size  $T$ , maximum number of iterations  $\bar{\ell}$ , number of CN updates to omit  $O$

1: **Training (Section III):**

- Build the neural network corresponding to the first window configuration with  $W$  and  $\bar{\ell}$ .
- Set the loss function that includes target nodes from positions 1 to  $T$ .
- At each training stage, train the CN weights  $w_{c_p}^{(\ell)}$  using actively collected samples, and validate the trained decoder using the normalized loss term.
- Repeat until the training converges

2: **Scheduling (Section IV):**

- Train the damping factors  $\gamma_{c_p}^{(\ell)}$ .
- Quantify the significance of each CN update based on the insignificance score  $\bar{\gamma}_{c_p}^{(\ell)}$ .
- Omit  $O$  CN updates with high insignificance score from the decoding process.

3: **Adaptive window decoding (Section V):**

- Build the neural network corresponding to the third window configuration.
  - Collect the training samples using the boosting learning technique.
  - Train the breakwater weight set  $\bar{w}_{c_p}^{(\ell)}$ .
  - If an error is not detected in the previous window, apply the plain weight set  $w_{c_p}^{(\ell)}$ .
  - Else, apply the breakwater weight set  $\bar{w}_{c_p}^{(\ell)}$ .
- 

EP without modifying the structure of the code or decoder, providing a benefit over conventional methods [30], [31].

The overall algorithm of the NWD is summarized in Alg. 1. The rest of the paper is organized as follows. Section II introduces the notation and background that are used throughout the paper. In Section III, we present the network structure of the NWD, benefits of target-specific training, and new training methods for fair training across multiple SNR points. In Section IV, we describe the neural non-uniform scheduling based on the training results of damping factors. The adaptive NWD, which selectively uses the breakwater weight set based on the previous error situation to mitigate EP, is presented in Section V. Finally, conclusion is given in Section VI.

## II. PRELIMINARIES

### A. SC-LDPC Codes and Window Decoding

In this paper, we consider protograph-based SC-LDPC codes [32]. The protograph of SC-LDPC codes is constructed by the edge-spreading technique to couple every  $w$  adjacent LDPC blocks out of a total of  $L$  disjoint LDPC blocks into a single coupled chain. The parameters  $w$  and  $L$  are called coupling width and chain length, respectively. The base matrix



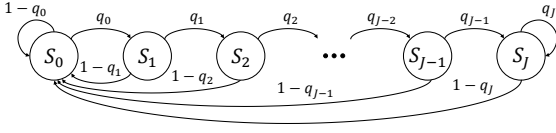


Fig. 3. A state transition diagram of a general Markov decoder model for window decoding process.

[34] and node-wise scheduling [35], dynamically changes the update order within each iteration. This results in a varying number of updates for each node by the end of the decoding process.

Unlike block LDPC codes, applying uniform serial schedules for window decoding of SC-LDPC codes proves ineffective in reducing complexity [33]. To address this, several non-uniform schedules specifically suited for window decoding are proposed in [29]. One approach utilizes estimated BER improvement. It calculates a soft BER estimate in each iteration and deactivates CN updates that are expected to provide minimal soft BER changes. These inactive CNs reuse messages from the previous iteration without updates. While this method achieves a significant reduction in CN updates (around 50%), it incurs a considerable overhead due to the real-time calculation of soft BER. Fig. 2 (a) shows a schedule obtained with this method, where boldly colored CNs represent those updated in each iteration.

To eliminate the overhead, the same study [29] proposes a pragmatic non-uniform scheduling that avoids additional calculations. This method deactivates a predetermined set of CN updates in a specific pattern, inspired by the results of the soft-BER based scheduling. Fig. 2 (b) shows the pragmatic schedule. Initially, all CNs are updated. In subsequent iterations, starting from the CN furthest from the target position, one CN is deactivated at a time. This process repeats after a period of  $W$  iterations. The pragmatic non-uniform schedule achieves substantial complexity reduction (35-40% fewer CN updates) without the need for additional calculations.

### C. Error Propagation in Window Decoding

As shown in Fig. 1(b), the decoding of the current window is influenced by the decision LLRs of previously processed VNs. Consequently, errors from prior stages can propagate, leading to a long chain of errors. EP is more prevalent in low-latency decoding settings that use a small window size  $W$  and a low maximum number of iterations  $\bar{\ell}$ . While these configurations are favorable for reducing latency, they also increase the likelihood of block errors and EP. The presence of EP significantly worsens the BLER and FER, especially when transmitting long or unterminated chains [24], [25].

To gain a deeper understanding of EP, a general Markov decoder model is introduced in [31]. Fig. 3 depicts the model's state transition diagram. Here, the index  $i$  of state  $S_i$  represents the number of consecutive block errors that occurred before the current window. Specifically,  $S_0$  indicates the state with no preceding errors, while  $S_i$  (for  $i = 1, 2, \dots, J - 1$ ) represent intermediate states where  $i$  consecutive windows resulted in

block errors. Finally,  $S_J$  represents a burst error state where more than  $J$  consecutive block errors have occurred. As the number of consecutive block errors increases due to EP, the error probability in the current window also rises. This is reflected in the transition probabilities, where  $q_{J-1} \geq q_{J-2} \geq \dots \geq q_1 \geq q_0$ . In simpler terms, a higher  $i$  value indicates a situation more susceptible to severe EP. Therefore, preventing error propagation from states with lower  $i$  becomes crucial.

### D. Neural Min-Sum Decoding

In this paper, we employ the neural min-sum decoding algorithm [9], which offers practical implementation with low decoding complexity while achieving performance close to the BP algorithm. Let  $m_{v \rightarrow c}^{(\ell)}$  ( $m_{c \rightarrow v}^{(\ell)}$ ) denote the message passed from VN  $v$  to CN  $c$  (and vice versa) during the  $\ell$ -th iteration. Initially, these messages are set as  $m_{v \rightarrow c}^0 = m_v^{\text{ch}}$ ,  $m_{c \rightarrow v}^0 = 0$ , where  $m_v^{\text{ch}}$  represents the channel LLR of VN  $v$ . For iteration  $\ell = 1, 2, \dots, \bar{\ell}$ , the neural min-sum algorithm updates the messages as follows:

$$m_{v \rightarrow c}^{(\ell)} = m_v^{\text{ch}} + \sum_{c' \in \mathcal{N}(v) \setminus c} m_{c' \rightarrow v}^{(\ell-1)} \quad (2)$$

$$m_{c \rightarrow v}^{(\ell)} = w_{c \rightarrow v}^{(\ell)} \left( \prod_{v' \in \mathcal{N}(c) \setminus v} \text{sgn}(m_{v' \rightarrow c}^{(\ell)}) \right) \min_{v' \in \mathcal{N}(c) \setminus v} |m_{v' \rightarrow c}^{(\ell)}|, \quad (3)$$

where  $\mathcal{N}(v)$  denotes the neighbors of node  $v$ . We refer to  $w_{c \rightarrow v}^{(\ell)}$  as CN weights as they attenuate CN messages. At the last iteration, the decision LLR  $m_v^0$  of VN  $v$  is calculated as

$$m_v^0 = m_v^{\text{ch}} + \sum_{c' \in \mathcal{N}(v)} m_{c' \rightarrow v}^{(\bar{\ell})}. \quad (4)$$

Note that the neural min-sum algorithm simplifies to the weighted min-sum algorithm [36] when CN weights share a single value  $\alpha$ .

Unlike the heuristically optimized weighted min-sum algorithm, the neural min-sum algorithm employs a plenty of weights that are optimized through machine learning techniques within a neural network. The neural network is constructed from the Tanner graph of codes. Fig. 4 shows an example of such neural network, which will be illustrated in detail in the next section. While the neural min-sum algorithm demonstrate superior performance compared to the weighted min-sum algorithm, assigning distinct weights to every edge incurs significant training complexity and memory requirements. To address this, various weight sharing techniques have been proposed, such as spatial sharing [10], protograph sharing, and CN sharing [11].

## III. NEURAL WINDOW DECODER FOR SC-LDPC CODES

This section introduces the NWD and its training methods. The NWD follows the window decoding process but incorporates CN weights similar to the neural decoding algorithm. Since the window configuration is repeated for each window stage, training the weights in the first window configuration is sufficient for reuse in subsequent stages. Thus, we focus on training the weights in the first window.

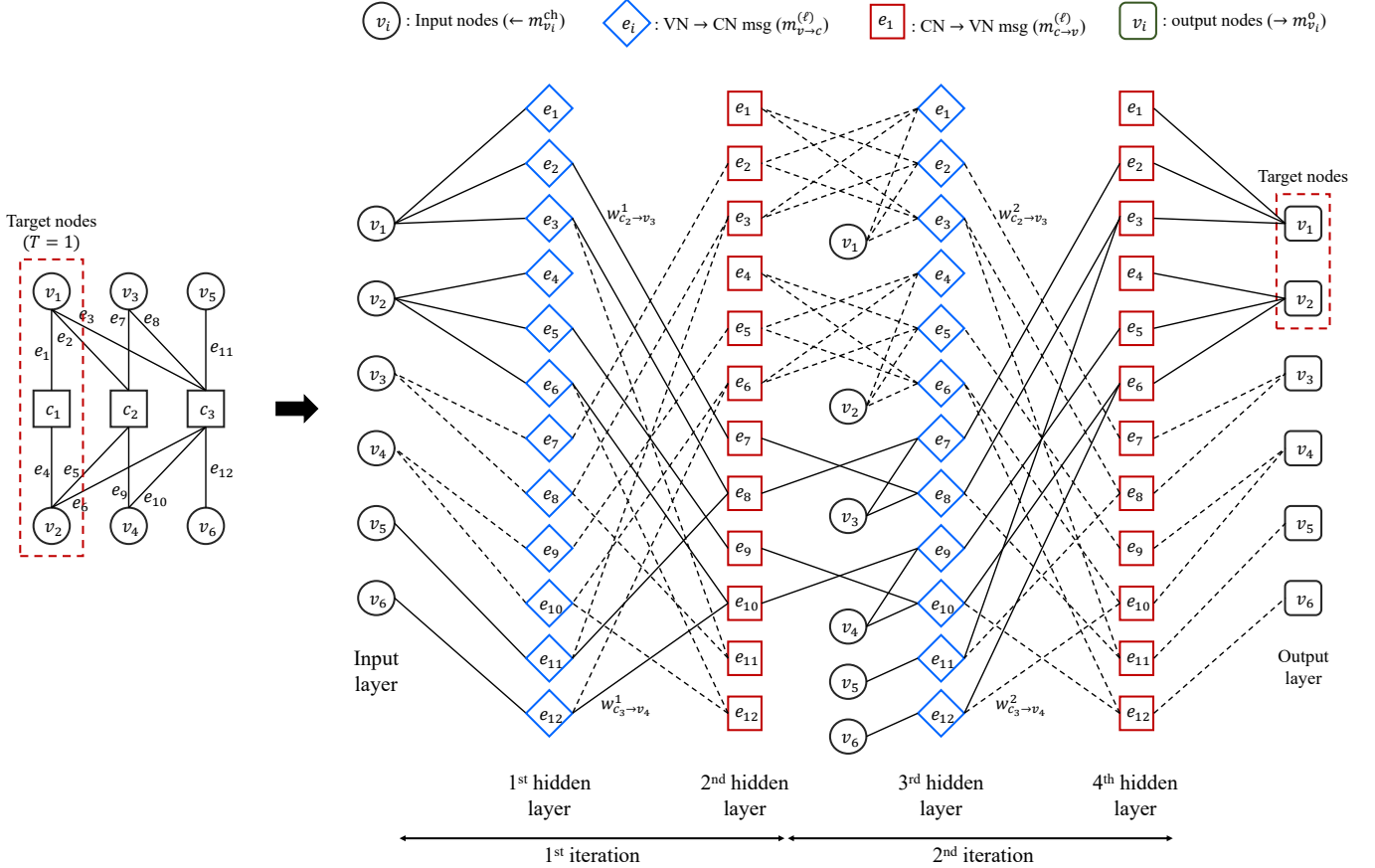


Fig. 4. The first window configuration with  $W = 3$  and  $\bar{\ell} = 2$  is mapped to the neural network for training the NWD. The dashed lines in the network represent edges that are included for all-inclusive training but are pruned for target-specific training.

### A. Target-Specific Training of NWD

The neural network for training the NWD is shown in Fig. 4. The first window configuration with  $W = 3$ ,  $z = 1$  and  $\bar{\ell} = 2$  is mapped to the neural network. It consists of  $WN_v$  input and output nodes, along with  $2 \times \bar{\ell}$  hidden layers. The nodes in the hidden layers do not directly correspond to VNs and CNs, but rather to the edges in the Tanner graph. The odd and even hidden layers perform the message updates of VNs in (2) and CNs in (3), respectively.

We employ weight sharing techniques to facilitate training. Since we focus on protograph-based SC-LDPC codes, protograph weight sharing [11] is primarily employed, assigning the same weight to edges corresponding to the same protograph edge. This method reduces the total number of trainable weights by a factor of  $1/z$ . Additionally, the CN-wise weight sharing technique [11] unifies weights assigned to the same proto CN. As a result, CN weights with weight sharing are represented as  $w_C^{(\ell)}$  for proto CN  $C$ . Thus, the number of trainable weights is reduced to  $Wn_c\bar{\ell}$ .

The loss function plays a crucial role in training the NWD. We consider the BLER loss term [28], which becomes 1 if a block error occurs and 0 otherwise, because achieving perfect block decoding within each window is essential to prevent EP. The original BLER loss term includes all output VNs in the neural network. All-inclusive training uses the loss term as

follows

$$L_A = \frac{1}{2} [1 - \text{sgn}(\min_{1 \leq v \leq WN_v} m_v^o)]. \quad (5)$$

However, given the window decoding process, we can restrict the loss term on target VNs and employ target-specific training. Let  $T (\leq W)$  denote the number of positions to be included in the loss term. The loss term for the target-specific training is given as

$$L_T = \frac{1}{2} [1 - \text{sgn}(\min_{1 \leq v \leq TN_v} m_v^o)]. \quad (6)$$

The neural network in Fig. 4 illustrates the pruning effect of target-specific training. All-inclusive training necessitates using all neural edges and nodes in the figure. In contrast, target-specific training with  $T = 1$  allows pruning the output VNs from  $v_3$  to  $v_6$  since they are not included in the loss term  $L_T$ . The dashed edges connected to these non-target nodes can be pruned, along with the connected nodes from  $e_7$  to  $e_{12}$  in the 4th hidden layer. This pruning process continues down to the input layer. In this example, target-specific training allows to eliminate 47% of nodes and 43% of edges.

As the edges of the neural network are pruned, the associated CN weights are also eliminated. In Fig. 5, we plot the ratio ( $A/B$ ) between the number of trainable weights for target-specific training ( $A$ ) and that for all-inclusive training ( $B$ ) according to the window size  $W$  and  $\bar{\ell}$ . As shown in Fig. 5(b),

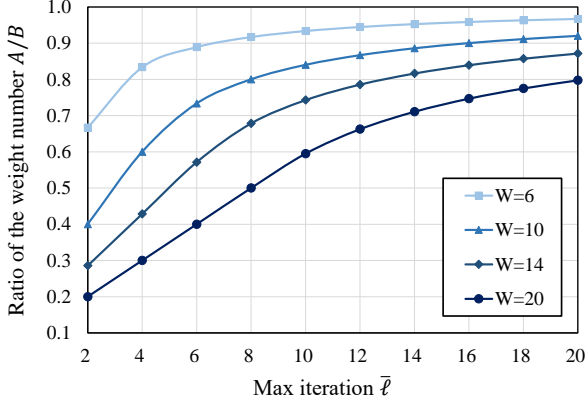


Fig. 5. Ratio between the numbers of trainable weights for target-specific training and all-inclusive training. A smaller ratio indicates a greater complexity reduction effect achieved by target-specific training.

larger the window size and smaller maximum iterations lead to a greater reduction in weights. For example, with  $W = 18$  and  $\bar{\ell} = 4$ , the weight ratio is 0.3, indicating that target-specific training reduces the number of weights by 70%.

It is important to note that target-specific training offers a greater reduction in low latency decoding scenarios. These scenarios typically involve a limited number of iterations per window stage to minimize decoding delay. The performance loss from fewer iterations can be compensated for by using a larger window size. Additionally, a larger window size is recommended to ensure sufficiently low BLER and prevent EP [37]. Therefore, Fig. 5 demonstrates that target-specific training is particularly advantageous in practical low-latency decoding scenarios.

### B. Proposed Training Methods across Multiple SNR Points

Now, we discuss about better methods of training neural decoders across multiple SNR points. Since the pioneering study of neural decoders by [7], most subsequent researches train neural decoders in the similar manner: Received words are collected from channels at various SNR points to form a mini-batch. After the designated number of training sessions using mini-batches, the training phase concludes and the validation phase begins. The score of the trained decoder is assessed using newly collected received words from the same SNR points. This process is repeated and the optimal neural decoder with the best score is selected in each stage. Since training occurs with new data each time, we refer to these repetitions as stages rather than epochs.

Conventionally, SNR points are selected at equal intervals, and a uniform number of data are gathered from each point to make a mini-batch. For example, a mini-batch with size 50 is formed by collecting 10 training data from each  $E_b/N_0$  point in  $\mathcal{S}_1 = \{0.6, 1.0, 1.4, 1.8, 2.2\}$ . However, this method makes training biased towards low SNR. Since it collects a uniform number of data at each point, the number of decoding errors from low SNR points significantly exceeds those from high SNR points. As the loss occurs only for decoding errors, most of the losses in one mini-batch come from low SNR data

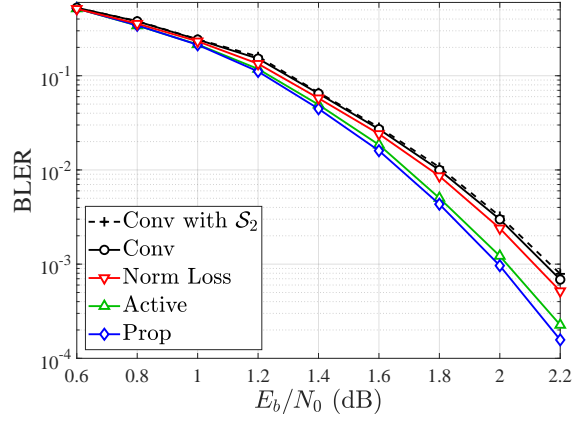


Fig. 6. BLER performance for  $W = 10$  window block of  $z = 100$  SC-LDPC code using  $\bar{\ell} = 10$  NWDs. The NWDs are trained using conventional method (Conv), normalized loss (Norm Loss), active learning (Active), and both methods combined (Prop). Training data are collected from  $\mathcal{S}_1$ , except the result of Conv with  $\mathcal{S}_2$ .

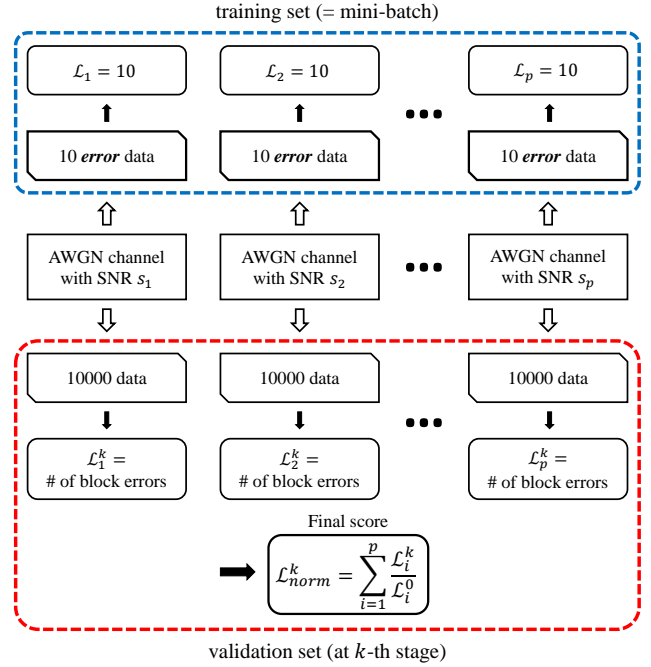


Fig. 7. Proposed training methods of neural decoders. Error data are selectively collected to construct a mini-batch, and normalized loss sum is employed as the final score for the validation set.

and thus the training is biased to them. In practice, an NWD trained with data from  $\mathcal{S}_1$  and an NWD trained with data from  $\mathcal{S}_2 = \{0.6, 1.0\}$  show almost no performance difference, as depicted in Fig. 6.

Therefore, instead of the conventional method, we adopt a simple *active learning* [15] method. To form mini-batches, we only collect the channel outputs that incur decoding errors at each SNR point, simply called error data. Since we utilize the BLER loss (6), we only collect data with a loss of 1. Therefore, in the above case of  $\mathcal{S}_1$ , using this active learning approach makes that the data from each SNR point  $s_p$  produces the same loss sum of  $\mathcal{L}_p = 10$ , ensuring data from each SNR



point equally contributes to the training.

Next, we propose a new method for calculating the final score of the trained decoder in each stage. The most common method is to simply sum BLERs (or losses) at each SNR point within the validation set, and we have verified that most of the open source codes for neural decoders to date use this method [9], [11], [17]. However, this approach also results in decoders that is biased to low SNR point. The performance of neural decoders typically improves multiplicatively from their initial untrained performance. Hence, low SNR data, which start with a high error rate, see larger improvements than high SNR data. For example, Improving the BLER  $0.2 \rightarrow 0.1$  at a low SNR point is scored 100 times higher than improving the BLER from  $0.002 \rightarrow 0.001$  at a high SNR point. Therefore, this method is likely to select decoders that perform better on low SNR point during the validation phase.

Therefore, instead of simply adding scores from each SNR points, we propose *normalized loss* sum as our final score, which first normalizes the losses with the initial losses of untrained decoders and then adds them. Assuming validation is conducted with data from  $E_b/N_0$  points  $\mathcal{S} = \{s_1, s_2, \dots, s_p\}$ , we denote the sum of losses for validation data from  $s_i$  in the  $k$ -th stage by  $\mathcal{L}_i^k$ . Then, the normalized loss sum for the  $k$ -th stage is presented as

$$\mathcal{L}_{norm}^k = \sum_{i=1}^p \frac{\mathcal{L}_i^k}{\mathcal{L}_i^0}. \quad (7)$$

Through this final score, we can assign the same score to a decoder that halves the BLER at low SNR and another that halves the BLER at high SNR. Fig. 7 presents an overview of the two proposed methods, when collecting 10 and 10000 data at each SNR point to form a mini-batch and a validation set, respectively.

The BLER improvement achieved by the two proposed methods is shown in Fig. 6. Among the two methods, active learning shows a greater improvement in BLER performance than the normalized loss. This is likely because the normalized loss is applied during the validation process, which is not directly related to the training itself.

Overall, we confirm that when training across a wide range of SNR points, applying both methods ensures stable training outcomes showing better performance. Additionally, it is meaningful that these methods guarantees results aligned with the intention of including multiple SNR points in the training range, preventing the training outcomes from being biased towards low SNR points as in the conventional method. We want to remark that both methods are not exclusive to NWD but are desirable to be applied when training general neural decoders for various SNR points.

### C. Training Results of NWD

Based on the methods discussed in the previous subsections, we train  $\bar{\ell} = 10, W = 10$  neural decoders for a  $z = 100$  SC-LDPC code. We employ PCN weight sharing and actively collect 20 error data from 5 SNR points in  $\mathcal{S} = \{1.2, 1.4, \dots, 2.0\}$  to form mini-batches of size 100. After 10 training sessions, the validation phase starts and the trained

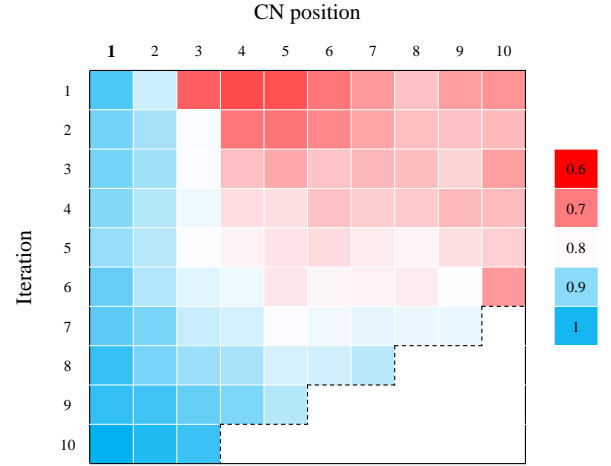


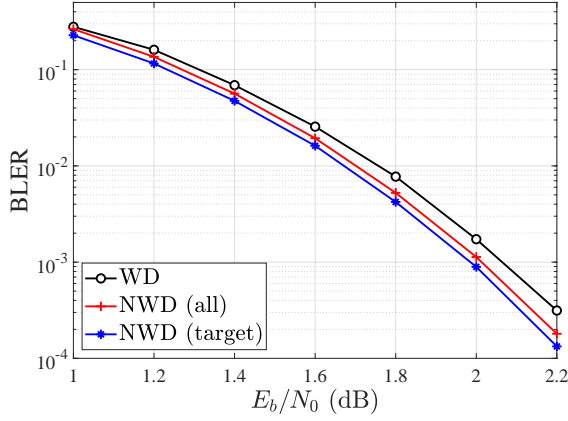
Fig. 8. Distribution of trained PCN weights in NWD with  $T = 1$  target-specific training by PCN position and iteration, with the target VNs at the bolded position 1. The small weights (red) signify that the corresponding CNs have low reliability.

weight set is evaluated using the normalized loss obtained from 50000 validation data. This entire process is repeated over 1000 stages, after which the best decoder is selected.

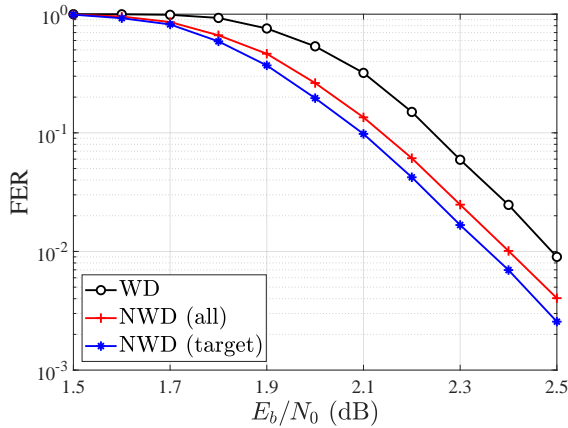
Fig. 8 displays a distribution of trained weights in NWD with  $T = 1$  target-specific training. The empty space under the dotted line indicate pruned weights that are not connected to target nodes. It shows that target-specific training reduces 16% weights compared to all-inclusive training. Weights trained to larger values indicate that the corresponding CNs are reliable in that iteration. Overall, weights that are closer to the target position and in the latter part of the iterations are trained to larger values. Since the training is conducted on a window, the front CNs have lower degrees and higher reliability than the rear CNs. As the iteration progresses, the reliability increases, supporting the weight pattern in the figure. However, when focusing on the early iterations, the weights of middle CNs are lower than those of the rear CNs (see PCNs 3 – 10 in iteration 1). The reason is that, in the rear, unreliable initial messages from high degree PCNs need more than 2 iterations to be transmitted to the target node, allowing for a natural recovery of reliability. However, in the middle, unreliable messages are transmitted directly to the target node, having more detrimental effect on target decoding.

Finally, Fig. 9 (a) shows the BLER performance for one window of trained NWDs, and conventional WD using a single weight of 0.75. NWD with target-specific training achieved a performance gain of 0.1 dB at a BLER  $= 3 \times 10^{-4}$  compared to WD, and shows a lower BLER than NWD with all-inclusive training even with fewer weights. The FER performances of the decoders with SC-LDPC code chain of  $L = 100$  is presented in Fig. 9 (b). The performance discrepancy widens as it goes through the  $L = 100$  chain, resulting in a larger FER gap than the BLER performance. NWD with target-specific training shows a performance gain of 0.15 dB at an FER  $= 10^{-2}$  compared to WD and also outperforms NWD with all-inclusive training.

Next, to better understand the effects of target-specific



(a)



(b)

Fig. 9. (a) BLER performances of a detached window block and (b) FER performances of a  $L = 100$  code for conventional WD, NWD with all-inclusive training, and NWD with  $T = 1$  target-specific training.

training, we examine the training progress of the NWDs. Fig. 10 shows the evolution of BLERs at SNR 1.4 dB for the NWDs with various target sizes. As the target size of the neural decoder decreases, continuous improvements occur, resulting in better performance convergence. This demonstrates that target-specific training with a small  $T$  enables deeper learning and achieves better performance despite having a simpler network and fewer weights compared to all-inclusive training.

#### IV. NEURAL NON-UNIFORM SCHEDULES FOR NWD

In this section, we propose a systematic method to optimize the non-uniform schedule based on the training result. In the non-uniform schedule, some CNs are deactivated and do not update their messages. The deactivated CNs transmit the same output as in the previous iteration.

##### A. Damping Factor and Insignificance Score

Determining which CNs to deactivate based solely on the trained CN weights  $w_C^{(\ell)}$  is challenging, as the weight values represent the reliability of the message, not the importance of the update itself. Therefore, we introduce damping factors

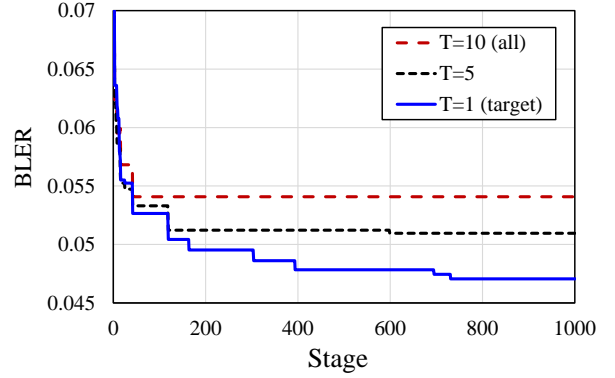


Fig. 10. Improvements of window BLER according to stages when training NWDs with various numbers of target sizes.

[10], [27] to the NWD, which directly reflect the importance of the current node update. Damping is a commonly used decoding technique that mixes the message of the current iteration with the message of the past iteration. The CN message with damping factors is as follows:

$$m_{c \rightarrow v}^{(\ell)} = \gamma_C^{(\ell)} m_{c \rightarrow v}^{(\ell-1)} + (1 - \gamma_C^{(\ell)}) m_{c \rightarrow v}^{(\ell)}, \quad (8)$$

where  $0 \leq \gamma_C^{(\ell)} \leq 1$  denotes the *damping factor* for PCN  $C$  at iteration  $\ell$ . The damped NWD incorporates the damping factors  $\gamma_C^{(\ell)}$  as trainable parameter along with the CN weights  $w_C^{(\ell)}$ . As in (8), a large damping factor implies that increasing the proportion of the previous message in the update is advantageous for decoding. Since deactivation is equivalent to setting  $\gamma_C^{(\ell)} = 1$ , deactivating CNs with high  $\gamma_C^{(\ell)}$  values first is expected to have minimal impact on decoding performance. To make as many  $\gamma_C^{(\ell)}$  values as close to 1 as possible, we introduce an L1 regularization term,  $\lambda \sum |1 - \gamma_C^{(\ell)}|$ , with  $\lambda = 0.1$  into the loss function of the damped NWD.

Fig. 11 (a) shows the distribution of trained  $\gamma_C^{(\ell)}$  values. In the initial iterations (up to 5), most  $\gamma_C^{(\ell)}$  values are concentrated in the range of 0-0.1 (colored blue to white), suggesting that updates to the corresponding CNs are essential. In the later iterations (iterations 7-10), larger  $\gamma_C^{(\ell)}$  values (red) appear, indicating that sufficient updates have been made by this point. Although the trained  $\gamma_C^{(\ell)}$  reflect the importance of CN updates, the presence of numerous similar small values makes it difficult to adequately select which CNs should be deactivated.

Therefore, we propose a new metric named the insignificance score  $\bar{\gamma}_C^{(\ell)}$ , defined as the damping factor  $\gamma_C^{(\ell)}$  divided by the normalized target reach count  $\bar{N}_C^{(\ell)}$ . Given the structure of SC-LDPC codes, the impact of CN deactivation on the target VNs varies significantly according to the distance to the target VNs. To account for this, we count the number  $N_C^{(\ell)}$  of paths each CN can reach the target VNs at the last iteration in the expanded trellis graph across iterations. For example, the first CN at iteration 9 has 6 paths to the target VNs at iteration 10 in the trellis graph, which means  $N_1^9 = 6$ . We normalize these counts within each iteration so that their sum equals 1



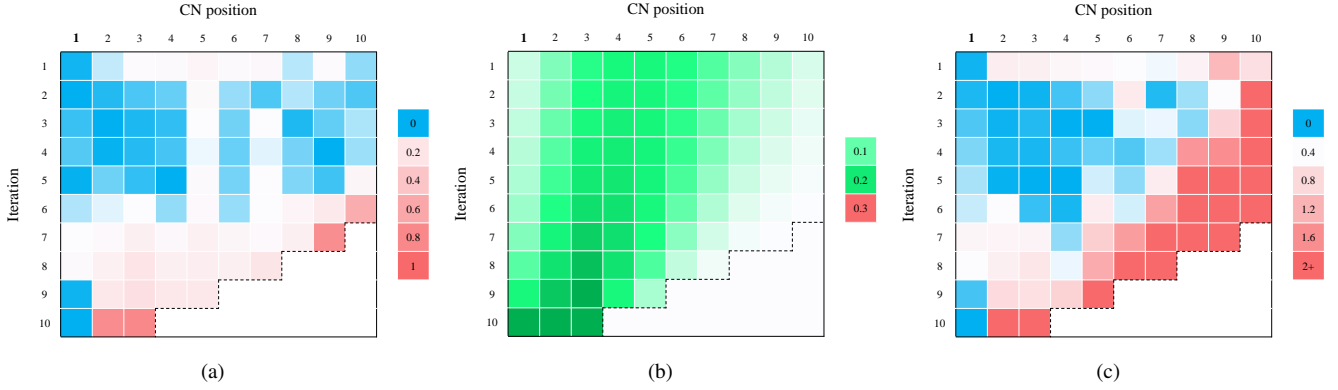


Fig. 11. (a) Distribution of trained damping factors  $\gamma$ , (b) normalized target reach counts  $\bar{N}$ , and (c) insignificance scores  $\bar{\gamma}$ . CN updates with a high insignificant score (red in (c)) is considered to be deactivated.

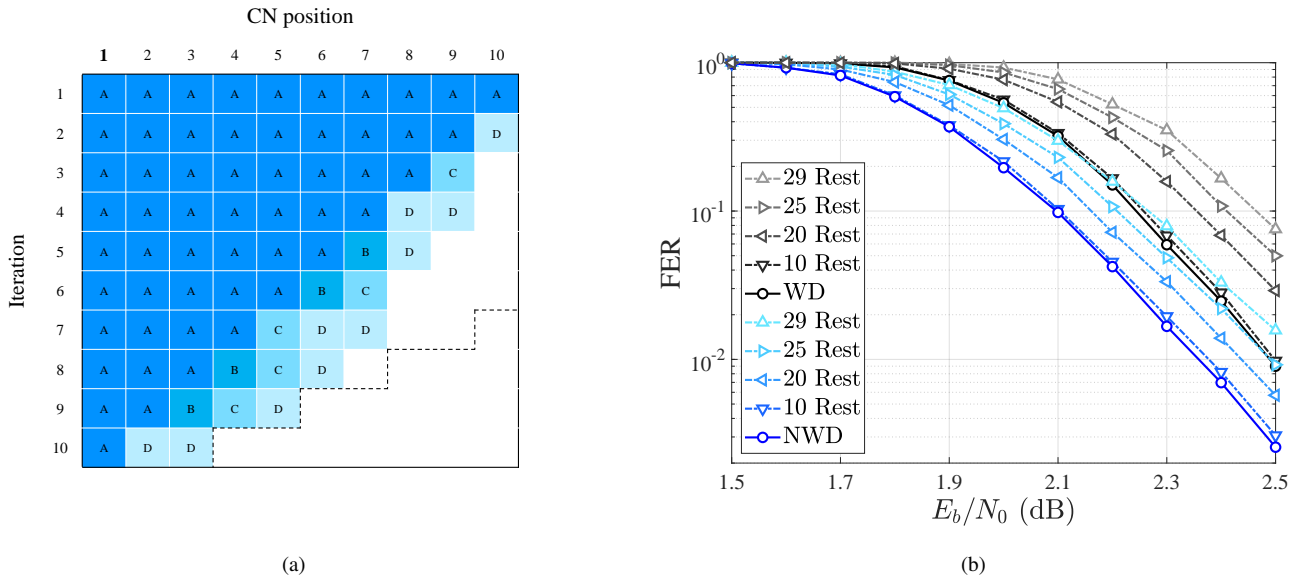


Fig. 12. (a) Non-uniform schedules based on the training results of the NWD: the points marked with 'A', 'A+B', 'A+B+C', and 'A+B+C+D' indicate the active CN updates when deactivating 29, 25, 20, and 10 CN updates, respectively. (b) FER performance with proposed neural non-uniform schedules applied to WD and NWD.

for each iteration. This normalized count  $\bar{N}_C^{(\ell)}$  represents the relative impact of a CN's update on the target VNs in each iteration. The distribution of normalized counts is shown in Fig. 11 (b).

Using these counts, we obtain the insignificance score  $\bar{\gamma}_C^{(\ell)} = \gamma_C^{(\ell)} / \bar{N}_C^{(\ell)}$ , as shown in Fig. 11(c). CNs with small insignificance scores are considered candidates for deactivation. Comparing the results in Fig. 11(a) and (c), the rear CNs at each iteration (e.g., iteration 4 and CN index 9), which have higher damping factors  $\gamma_C^{(\ell)}$ , are highly likely to be deactivated because they have fewer paths to the target VNs and thus have higher insignificance scores  $\bar{\gamma}_C^{(\ell)}$ . Deactivating CNs with high insignificance scores has little impact on the reliability of the target VNs and leads to less degradation of decoding performance.

### B. Proposed Non-Uniform Schedules of NWD

We deactivate CNs one by one according to the following rule. First, collect the insignificance scores  $\bar{\gamma}_C^{(\ell)}$  of the last active iterations across all positions. Then, deactivate one CN with the largest  $\bar{\gamma}_C^{(\ell)}$  at a time. The resulting schedules are shown in Fig. 12 (a) for cases where 29, 25, 20, and 10 CNs are deactivated. Points marked with the symbol 'A' indicate the active CNs when 29 CNs are deactivated, while 'A+B' marks the active CNs when 20 CNs are deactivated, and so on.

We determine schedules based on the trained damping factors of the damped NWD. However, decoding with the damping technique requires additional memory to store all previous messages  $m_{c \rightarrow v}^{(\ell-1)}$  as described in equation (8). This significantly increases memory requirements and decoding complexity, potentially negating the complexity reduction benefits achieved by scheduling. Therefore, we use the damped NWD only to determine the schedule, and the actual de-

coding is performed using the plain NWD with the established schedule. In practice, we confirm that the performance achieved by the plain NWD is nearly indistinguishable from that achieved by the damped NWD. Therefore, applying the proposed scheduling incurs no overhead, allowing the NWD to fully benefit from the reduction in complexity.

Fig. 12 (b) presents the FER performance of the NWD and WD with the schedules in Fig. 12 (a). For the NWD, we observe that the schedule with 10 inactive CNs, resulting in a 26% reduction in CN updates, has almost no performance loss. Moreover, the performance of the NWD with 25 inactive CNs surpasses that of the conventional WD, suggesting that using the NWD with an appropriate scheduling method can achieve comparable performance to the conventional decoder while omitting 41% CN updates. For the WD, performance degradation is minimal up to 10 inactive CNs, but beyond that, it experiences greater performance degradation than the NWD. This implies that the proposed scheduling method combines well with the NWD as intended.

Note that the schedule with 29 inactive CNs aligns with the pragmatic schedule in [29]. While the pragmatic schedule provides only one option of scheduling that could lead to performance loss as shown in Fig. 12 (b), the proposed method offers various options within the trade-off relationship between decoding complexity and decoding performance. Through neural non-uniform scheduling, one can flexibly achieve the desired balance between decoding complexity and decoding performance. It is notable that the proposed method is applicable not only to SC-LDPC codes but also to any codes with structural asymmetry in decoding influence.

## V. ADAPTIVE NWD FOR MITIGATING ERROR PROPAGATION

Up to this point, the training of the NWD has been conducted in the first window configuration. However, the trained weights are not suitable for subsequent window stages if errors occur in previous stages. Incoming messages from the processed VNs, shown as red edges in Fig. 8, could be erroneous. While the first window configuration has reliable messages on the left side, EP reverses the situation, making the front nodes the most unreliable. Therefore, although the NWD performs well in scenarios where decoding continues to be successful, it tends to be vulnerable to EP cases.

The general Markov decoder model in Fig. 3 [31] shows that it becomes more difficult to escape from EP as the decoder reaches deeper EP states. Thus, a simple yet effective method to mitigate EP is to prevent it immediately at the current stage when an error is detected in the previous stage. Hence, we focus on the model with  $J = 1$  in Fig. 3 and aim to lower the probability  $q_1$  to aid the decoder immediately escape from state  $S_1$ . We refer to  $q_1$ , the probability that an error occurs in the current block given that an error occurred in the previous block, as the *EP probability*.

### A. Training Method of Breakwater Weight Set

We propose an adaptive NWD scheme that use the plain weight set  $w_{c_p}^{(\ell)}$  and switches to a breakwater weight set  $\bar{w}_{c_p}^{(\ell)}$

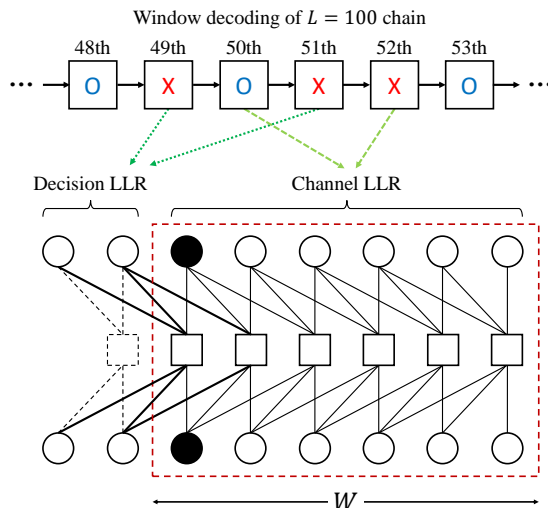


Fig. 13. The training method for the breakwater weight set. If error occurs in the previous block (49, 51), the decision LLRs of the target VNs from the previous block and the channel LLRs of all VNs from the current block (50, 52) are gathered as training data.

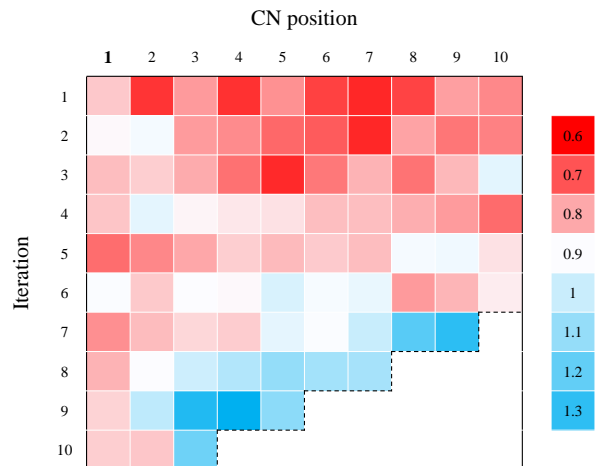


Fig. 14. Distribution of the trained breakwater weight set.

when an error is detected in the previous stage. While the plain weight set  $w_{c_p}^{(\ell)}$  is trained in the neural network corresponding the first window configuration, the breakwater weight set  $\bar{w}_{c_p}^{(\ell)}$  is trained in the neural network corresponding to the third window configuration that also include the processed VNs connected to the front CNs, as shown in Fig. 13. This accounts for situations where errors are propagated from the previous stage.

To collect training samples for  $\bar{w}_{c_p}^{(\ell)}$ , we utilize the boosting learning technique [17], which selectively collects uncorrected words from the previous decoder in a multi-stage decoding scenario. Similarly, we collect training samples in scenarios where errors occurred with the NWD. For example, as shown in Fig. 13, if an error occurs at the 50th window stage, we collect the decision LLRs of VNs in position 50 and the received LLRs of VNs belonging to the 51st window configuration. A total of 5000 training samples are collected

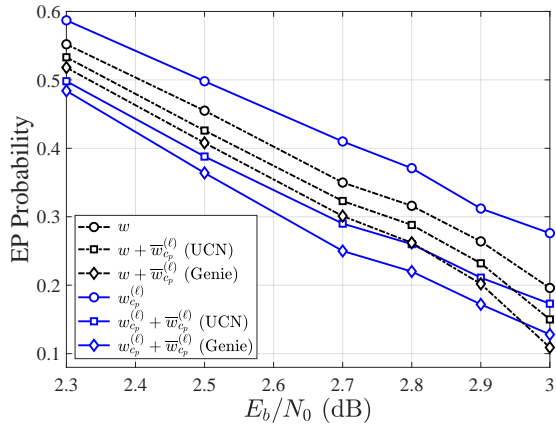


Fig. 15. EP probabilities for WD ( $w$ ), NWD ( $w_{c_p}^{(\ell)}$ ), and various adaptive NWDs. Adaptive NWDs detect errors in the previous block based on the unsatisfied status of the previous CN (UCN) or using a genie-aided (Genie) approach.

at an SNR point of 2.0 dB, and training is performed for 500 epochs. The initial weights are set using the plain weight set. Before training, the EP probability is 0.781, and after training, it is reduced to 0.642, indicating that the breakwater weight set is better at combating to the EP situation.

The distribution of  $\bar{w}_{c_p}^{(\ell)}$  is depicted in Fig. 14. Compared to the distribution of the plain weight set  $w_{c_p}^{(\ell)}$  in Fig. 8, it is evident that the front CN weights are trained with significantly smaller values due to the unreliable incoming messages. Conversely, in the latter iterations of mid-to-rear CNs, trained weights are greater than 1, indicating that messages from the relatively more reliable rear nodes need to be strengthened to correct errors flowing from the front.

### B. Proposed Adaptive NWD Scheme

The adaptive NWD scheme needs to detect whether an error occurs in the previous stage. One method for detecting errors is utilizing the parity check equations of CNs connected solely to the previously decoded target VNs (see dashed square in Fig. 13). If any unsatisfied CN (UCN) is found by checking the parity check equations, we consider it an indication of a previous stage error and use the breakwater weights for decoding the current stage. Due to the symmetric structure of SC-LDPC codes, the VNs at the top and bottom always have the same values in finite-length codewords. If the UCN occurs, it indicates that there is an odd number of 1s in the previous target VNs, which necessarily means that at least one error has occurred. In addition to the UCN method, we also evaluate a genie-aided method for error detection.

Fig. 15 shows the average EP probability across all positions. First, comparing the NWD and WD, we can observe that the NWD has a higher EP probability. This is because the NWD is trained in a situation without EP. On the other hand, by using the adaptive NWD scheme, the EP probability can be significantly reduced. The UCN detection method also shows a similarly low EP probability, close to that of genie-aided detection. The difference becomes more pronounced

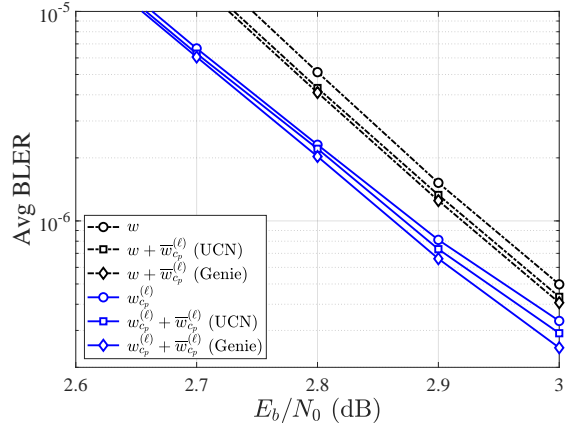


Fig. 16. Average BLER performances of a  $L = 100$  SC-LDPC code for WD, NWD, and various adaptive NWDs.

in the high SNR regions where the discrepancy between EP cases and error-free cases is more significant [31]. This demonstrates that NWD is more vulnerable to EP situations than WD. In contrast, adaptive NWD based on UCN detection successfully addresses EP cases, resulting in a lower EP probability than WD. Furthermore, if the previous block errors are accurately detected by a genie-aided approach, the EP probability is further reduced. For comparison, we also observe the performance of adaptive NWD applying fixed weight of 0.75 instead of the plain weight set  $w_{c_p}^{(\ell)}$  in error-free cases. In this scenario, the decision LLRs coming from WD differ from the training samples of the breakwater weight set, leading to a less effective reduction in EP probability compared to  $w_{c_p}^{(\ell)} + \bar{w}_{c_p}^{(\ell)}$ .

Finally, we compare the average BLER performance of the SC-LDPC code with  $L = 100$  using various decoders in Fig. 16. When comparing the NWD and WD, since the EP probability of the NWD worsens as we move to higher SNR, the NWD suffers from a more gradual slope of the BLER curve. However, the adaptive NWD scheme improves the EP probability and restores the slope at high SNR to levels comparable to WD.

Overall, while the adaptive NWD scheme shows a modest performance gain, its minimal overhead makes it worth considering for practical applications. Unlike previous methods to mitigate EP that require code modification [31] or changes of the decoder structure [30], the adaptive NWD scheme addresses EP by simply adding one more weight set to memory. Moreover, block error detector based on UCNs has a negligible impact on decoding latency and complexity.

## VI. CONCLUSION

In this paper, we discussed NWD and its derivative techniques for SC-LDPC codes. Firstly, we observed that target-specific training not only reduces the number of weights, thereby decreasing training complexity and memory requirements, but also enhances decoding performance. For the training of NWD, we collected error data samples from multiple SNR points, and utilized normalized loss in the validation

process to prevent training from being biased towards specific SNR points. The trained NWD achieved the better performance than the conventional WD and the NWD with all-inclusive training, even with fewer weights. Secondly, we proposed a neural non-uniform schedule based on the training results of damped NWD. The schedule combined with NWD achieved better performance than WD with only 59% of the CN updates. Lastly, we proposed an adaptive NWD that employs breakwater NWD based on the error occurrence in the previous block to mitigate EP. Adaptive NWD successfully improved both EP probability and BLER without requiring changes of the decoder or code structure. Overall, it is notable that the proposed methods are highly hardware-friendly and involve minimal overhead, as they require only the addition of weights to the existing decoder once training has completed. Therefore, the proposed NWD can be practically implemented and directly used for decoding SC-LDPC codes.

## REFERENCES

- [1] H. He, C.-K. Wen, S. Jin, and G. Y. Li, "Deep learning-based channel estimation for beamspace mmWave massive MIMO systems," *IEEE Wireless Commun. Lett.*, vol. 7, no. 5, pp. 852–855, Oct. 2018.
- [2] T. O'Shea and J. Hoydis, "An introduction to deep learning for the physical layer," *IEEE Trans. Cognitive Commun. Netw.*, vol. 3, no. 4, pp. 563–575, Dec. 2017.
- [3] K. Muah, R. Fritschek, and R. F. Schaefer, "Learning End-to-End Channel Coding with Diffusion Models," in *WSA & SCC 2023; 26th International ITG Workshop on Smart Antennas and 13th Conference on Systems, Communications, and Coding*, 2023, pp. 1–6.
- [4] W. R. Caid and R. W. Means, "Neural network error correcting decoders for block and convolutional codes," in *Proc. IEEE Global Telecommunications Conference and Exhibition (GLOBECOM)*, 1990, pp. 1028–1031.
- [5] L. G. Tallini and P. Cull, "Neural nets for decoding error-correcting codes," in *Proc. IEEE Tech. Appl. Conf. Workshops*, 1995, p. 89.
- [6] T. Gruber, S. Cammerer, J. Hoydis, and S. ten Brink, "On deep learning-based channel decoding," in *Proc. Annu. Conf. Inf. Sci. Syst. (CISS)*, 2017, pp. 1–6.
- [7] E. Nachmani, Y. Be'ery, and D. Burshtein, "Learning to decode linear codes using deep learning," in *Proc. 54th Annu. Allerton Conf. Commun., Control, Comput. (Allerton)*, Sep. 2016, pp. 341–346.
- [8] E. Nachmani, E. Marciano, D. Burshtein, and Y. Be'ery, "RNN decoding of linear block codes," 2017, *arXiv:1702.07560*.
- [9] E. Nachmani, E. Marciano, L. Lugosch, W. J. Gross, D. Burshtein, and Y. Be'ery, "Deep learning methods for improved decoding of linear codes," *IEEE J. Sel. Topics Signal Process.*, vol. 12, no. 1, pp. 119–131, Feb. 2018.
- [10] M. Lian, F. Carpi, C. Häger, and H. D. Pfister, "Learned belief-propagation decoding with simple scaling and SNR adaptation," in *Proc. IEEE Int. Symp. Inf. Theory (ISIT)*, Jul. 2019, pp. 161–165.
- [11] J. Dai, K. Tan, Z. Si, K. Niu, M. Chen, H. V. Poor, and S. Cui, "Learning to decode protograph LDPC codes," *IEEE Journal on Selected Areas in Communications*, vol. 39, no. 7, pp. 1983–1999, May 2021.
- [12] L. Wang, C. Terrill, D. Divsalar, and R. D. Wesel, "LDPC decoding with degree-specific neural message weights and RCQ decoding," *IEEE Transactions on Communications*, vol. 72, no. 4, pp. 1912–1924, Apr. 2024.
- [13] X. Chen and M. Ye, "Cyclically equivariant neural decoders for cyclic codes," in *Proc. International Conference on Machine Learning (ICML)*, 2021.
- [14] E. Nachmani, and L. Wolf, "Hyper-graph-network decoders for block codes," *Advances in Neural Information Processing Systems*, vol. 32, 2019.
- [15] I. Be'ery, N. Raviv, T. Raviv, and Y. Be'ery, "Active deep decoding of linear codes," *IEEE Transactions on Communications*, vol. 68, no. 2, pp. 728–736, 2020.
- [16] A. Buchberger, C. Hager, H. D. Pfister, L. Schmalen, and A. Graell I Amat, "Pruning and quantizing neural belief propagation decoders," *IEEE J. Sel. Areas Commun.*, vol. 39, no. 7, pp. 1957–1966, 2020.
- [17] H. Y. Kwak, D. Y. Yun, Y. Kim, S. H. Kim, and J. S. No, "Boosting Learning for LDPC Codes to Improve the Error-Floor Performance," *Advances in Neural Information Processing Systems (NeurIPS)*, vol. 36, 2024.
- [18] N. Shah and Y. Vasavada, "Neural layered decoding of 5G LDPC codes," *IEEE Commun. Lett.*, vol. 25, no. 11, pp. 3590–3593, 2021.
- [19] H. Y. Kwak, J. W. Kim, Y. Kim, S. H. Kim, and J. S. No, "Neural Min-Sum Decoding for Generalized LDPC Codes," *IEEE Communications Letters*, vol. 26, no. 12, pp. 2841–2845, 2022.
- [20] W. Xu, X. Tan, Y. Be'ery, Y. L. Ueng, Y. Huang, X. You, and C. Zhang, "Deep learning-aided belief propagation decoder for polar codes," *IEEE Journal on Emerging and Selected Topics in Circuits and Systems*, vol. 10, no. 2, pp. 189–203, 2020.
- [21] A. Jiménez Felström and K. S. Zigangirov, "Time-varying periodic convolutional codes with low-density parity-check matrix," *IEEE Trans. Inf. Theory*, vol. 45, no. 6, pp. 2181–2191, Sep. 1999.
- [22] S. Kudekar, T. J. Richardson, and R. L. Urbanke, "Threshold saturation via spatial coupling: why convolutional LDPC ensembles perform so well over the BEC," *IEEE Trans. Inf. Theory*, vol. 57, no. 2, pp. 803–834, Feb. 2011.
- [23] A. R. Iyengar, M. Papaleo, P. H. Siegel, J. K. Wolf, A. Vanelli-Coralli, and G. E. Corazza, "Windowed decoding of protograph-based LDPC convolutional codes over erasure channels," *IEEE Trans. Inf. Theory*, vol. 58, no. 4, pp. 2303–2320, Apr. 2012.
- [24] M. Zhu, D. G. M. Mitchell, M. Lentmaier, D. J. Costello, Jr., and B. Bai, "Combating error propagation in window decoding of braided convolutional codes," in *Proc. IEEE International Symposium on Information Theory (ISIT)*, USA, June. 2018, pp. 1380–1384.
- [25] M. Zhu, D. G. M. Mitchell, M. Lentmaier, D. J. Costello, Jr., and B. Bai, "Error propagation mitigation in sliding window decoding of braided convolutional codes," *IEEE Trans. Commun.*, vol. 68, no. 11, pp. 6683–6698, Nov. 2020.
- [26] D. E. Rumelhart, G. Hinton, and R. J. Williams, "Learning representations by back-propagating errors," *nature*, vol. 323, no. 6088, pp. 533–536, 1986
- [27] M. Fossorier, R. Palanki, and J. Yedidia, "Iterative decoding of multi-step majority logic decodable codes," in *Proc. Int. Symp. on Turbo Codes & Iterative Inform. Proc.*, 2003, pp. 125–132.
- [28] X. Xiao, N. Raveendran, B. Vasic, S. Lin, and R. Tandon, "FAID diversity via neural networks," in *Proc. 11th Int. Symp. Topics Coding (ISTC)*, Aug. 2021, pp. 1–5.
- [29] N. UI Hassan, A. E. Pusane, M. Lentmaier, G. P. Fettweis, and D. J. Costello, Jr., "Non-uniform window decoding schedules for spatially coupled LDPC codes," *IEEE Transactions on Communications*, vol. 65, no. 2, pp. 501–510, Feb. 2017.
- [30] K. Kläiber, S. Cammerer, L. Schmalen, and S. ten Brink, "Avoiding burst-like error patterns in windowed decoding of spatially coupled LDPC codes," in *Proc. IEEE 10th Int. Symp. on Turbo Codes & Iterative Inf. Processing*, Hong Kong, China, Dec. 2018, pp. 1–5.
- [31] M. Zhu, D. G. M. Mitchell, M. Lentmaier, D. J. Costello, Jr., and B. Bai, "Error propagation mitigation in sliding window decoding of spatially coupled LDPC codes," *IEEE Journal on Selected Areas in Information Theory*, 2023.
- [32] D. G. M. Mitchell, M. Lentmaier, and D. J. Costello, Jr., "Spatially coupled LDPC codes constructed from protographs," *IEEE Trans. Inf. Theory*, vol. 61, no. 9, pp. 4866–4889, July. 2015.
- [33] E. Sharon, N. Presman, and S. Litsyn, "Convergence analysis of generalized serial message-passing schedules," *IEEE J. Sel. Areas Commun.*, vol. 27, no. 6, pp. 1013–1024, Aug. 2009.
- [34] G. Elidan, I. McGraw, and D. Koller. (Jul. 2006), "Residual belief propagation: Informed scheduling for asynchronous message passing," [Online]. Available: <https://arxiv.org/abs/1206.6837>
- [35] A. I. V. Casado, M. Griot, and R. D. Wesel, "LDPC decoders with informed dynamic scheduling," *IEEE Trans. Commun.*, vol. 58, no. 12, pp. 3470–3479, Dec. 2010.
- [36] J. Chen, A. Dholakia, E. Eleftheriou, M. P. C. Fossorier, and X.-Y. Hu, "Reduced-complexity decoding of LDPC codes," *IEEE Trans. Commun.*, vol. 53, no. 8, pp. 1288–1299, Aug. 2005.
- [37] K. Huang, D. G. M. Mitchell, L. Wei, X. Ma, and D. J. Costello, Jr., "Performance comparison of LDPC block and spatially coupled codes over GF(q)," *IEEE Trans. Commun.*, vol. 63, no. 3, pp. 592–604, Mar. 2015.